Eye (2021) 35:1228–1234
https://doi.org/10.1038/s41433-020-1067-x

The ROYAL COLLEGE of OPHTHALMOLOGISTS

ARTICLE

Peripapillary hyperreflective ovoid mass-like structures—a novel entity as frequent cause of pseudopapilloedema in children

Daphna Mezad-Koursh[1,2] · Ainat Klein[1,2] · Amir Rosenblatt[1,2] · Sharon Teper Roth[2] · Meira Neudorfer[1,2] · Anat Loewenstein[1,2] · Matias Iglicki[3] · Dinah Zur[1,2]

Received: 1 January 2020 / Revised: 20 June 2020 / Accepted: 23 June 2020 / Published online: 2 July 2020

Abstract

Background Optic nerve head drusen (ONHD) are considered the most common cause for pseudopapilloedema in children. We aimed to investigate and further characterize a new type of optic nerve head lesion on enhanced depth imaging optical coherence tomography (EDI-OCT) named peripapillary hyperreflective ovoid mass-like structures (PHOMS), and ONHD in asymptomatic children with pseudopapilloedema.

Methods Retrospective cohort study including 64 eyes from 32 patients with pseudopapilloedema due to PHOMS and/or ONHD. Mean age was 9.0 ± 3.1 years. PHOMS and ONHD were identified and classified on EDI-OCT and infrared images. Ultrasound images were classified for the presence of hyperechogenic structures of the optic nerve head.

Results On EDI-OCT, PHOMS were detected in 63 out of 64 eyes (98.4%). In 60 eyes (93.8%), small hyperreflective foci inside the PHOMS were present. In all cases, we identified a new ring sign visible on infrared images, corresponding clearly to the edge of the PHOMS as seen on EDI-OCT. On ultrasound, we describe a new feature of PHOMS appearing as small hyperechogenic structures without posterior shadowing. In 13 eyes (20.3%), ONHD were present on EDI-OCT and ultrasound.

Conclusion This is the first study showing that PHOMS are the most common cause for pseudopapilloedema in children. PHOMS is a new entity of optic nerve head lesions. It might be a precursor of buried optic nerve head drusen, which can lead to visual field defects, haemorrhages and CNV. This study offers new tools to identify and follow-up these lesions early in childhood using EDI-OCT.

Introduction

Suspected papilloedema is a common cause for referral of children, while the vast majority of cases turn out to be pseudopapilloedema, caused by optic nerve head drusen (ONHD) [1, 2]. Misdiagnosing ONHD as disc oedema may lead to extensive, invasive, cost intensive and unnecessary workup and cause needless patient anxiety [3, 4]. The prevalence of ONHD in the paediatric population is about 0.4% [5], compared to 2.4% in adults [6]. This difference is probably due to the deeper location of the drusen in children [5–8]. Buried drusen located closer to the lamina cribrosa, which cause pseudopapilloedema are more difficult to appreciate clinically, frequently requiring imaging for confirmatory diagnosis [9].

B-scan ultrasound is considered the gold standard to diagnose ONHD [10], though spectral-domain optical coherence tomography (SD-OCT) and the addition of enhanced depth imaging (EDI) enable high resolution visualization of ONHD, their internal characteristics, and relationship to the lamina cribrosa [9, 11–14]. Ultrasound and enhanced depth imaging optical coherence tomography (EDI-OCT) have an equal detection rate of ONHD in clinically obvious cases in adults. In contrast, in cases that did not show obvious signs of ONHD in clinical exam,

These authors contributed equally: Daphna Mezad-Koursh, Ainat Klein

✉ Dinah Zur
dinahzur@gmail.com

[1] Division of Ophthalmology, Tel Aviv Sourasky Medical Center, Tel Aviv, Israel

[2] Sackler Faculty of Medicine, Tel Aviv University, Tel Aviv, Israel

[3] Private Retina Office, University of Buenos Aires, Buenos Aires, Argentina

ultrasound and non-EDI-OCT missed drusen in 11.8%, while EDI-OCT detected all cases [15]. The lack of standardization and conflicting descriptions and classifications of ONHD morphology on EDI-OCT have led to confusion amongst physicians and diverging results [9, 13, 16–19].

Lately, *The Optic Disc Drusen Studies Consortium* identified an additional type of optic nerve head lesion, considered distinct from traditional ONHD [14]. Previously classified as subretinal hyperreflective ONHD or mass lesions [11, 13, 17–19], these are now labelled 'Peripapillary hyperreflective ovoid mass-like structures' (PHOMS). It was suggested that this entity should not be included as a diagnostic criterion of ONHD. Although the definition of *The Optic Disc Drusen Studies Consortium* provides a standardized tool to correctly diagnose drusen, the entity of PHOMS is based on a sample of 28 cases above the age of 18 years.

To our best knowledge, PHOMS characteristics have not been described in a comprehensive manner in a paediatric population. The aim of our study was to investigate and further characterize PHOMS and ONHD in asymptomatic children with pseudopapilloedema using EDI-OCT and ultrasound.

Methods

This retrospective descriptive study was performed at the Tel Aviv Medical Center, Tel Aviv, Israel. Institutional Review Board approval was obtained. The study adhered to the tenets of the Declaration of Helsinki. There was no need for informed consent.

Study participants

The study consisted of consecutive eyes from children (aged 5–16 years) referred with an accidental clinical finding of suspected pseudopapilloedema, seen between September 2015 and January 2019. All patients that had ONHD and/or PHOMS confirmed by EDI SD-OCT imaging of the optic nerve head available at time of diagnosis and had undergone B-scan ultrasound were included. Children with true disc oedema were excluded from the study, when there was clinical evidence of disc swelling on biomicroscopy, thickening of the retinal nerve fibre layer on OCT, or evidence of excess optic nerve sheath fluid on ultrasound [20]. Patients' charts were reviewed for demographic and clinical data including age, gender, affected eye, medical and ocular history.

EDI-OCT

All EDI-OCT scans were obtained using the Heidelberg Spectralis (Heidelberg Engineering, Heidelberg, Germany) with a dense horizontal raster (15 × 10°, 97 sections) [14] centred on the optic nerve head and graded by two masked assessors (DZ and MI). In case of disagreement, the image was graded by a third senior observer (MN). PHOMS and ONHD were graded on EDI-OCT according to the recommendations of *The Optic Disc Drusen Studies Consortium* [14]:

(1) Presence of ONHD: hyporeflective structures with a full or partial hyperreflective margin.
(2) Presence of PHOMS: hyperreflective structures located external to and surrounding large parts of the disc.
(3) PHOMS size: quantitatively assessed as maximal vertical height measured perpendicular to the retinal pigment epithelium (in μm) using the calliper tool of the instrument [11].

Ultrasound

In total, 10 MHz B-scan ultrasound images were obtained using the Aviso S (Quantel Medical, Clermont-Ferrand, France) and analysed by two masked assessors (DZ and MI). Ultrasound images were evaluated for the following parameters:

(1) Presence of hyperechogenic structures.
(2) Size of hyperechogenic structures—measured using the calliper tool of the instrument at a gain of 90 dB. The extent of the hyperechogenic component displayed parallel to the retina was measured (in mm).
(3) Minimal gain required to display the hyperechogenic structure (in dB).

Fundus autofluorescence

Fundus autofluorescence (FAF) images were obtained using Heidelberg Spectralis (Heidelberg Engineering, Heidelberg, Germany). FAF images of the optic nerve head were evaluated for presence of small hyper AF spots or confluent hyper AF areas.

Statistical analysis

Data were recorded in Microsoft Excel and analysed using SPSS version 25 (SPSS Inc., Chicago, IL, USA). Continuous variables were compared between subjects using the independent sample *t*-test. For small group comparison and ordinal variables, Mann–Whitney *U*-test was used. To analyse correlation between continuous variables the Pearson's correlation test was used. Binary variables were compared within

subjects using the McNemar test for symmetry and between subjects using The Fisher's exact test or Pearson chi-square test to explore categorical variables. In this case, due to the lack of undetected drusen on OCT a theoretical undetected drusen was added to both groups and was negligibly weighted, thus negating its effect on statistical analysis. All tests were two tailed, and the threshold for statistical significance was defined as a p value < 0.05. Interrater reliability was tested as absolute agreement with a two-way mixed interclass correlation model.

Results

Thirty-nine asymptomatic children were referred due to an incidental finding of suspected pseudopapilloedema during routine examination. A total 32 children were included, all identified in a consecutive manner. Mean patient age was 9.0 ± 3.1 years (range 5–16). Demographic data and descriptive statistics are shown in Table 1.

Seven children were diagnosed with true papilloedema and excluded from the study. In these cases, ultrasound showed excess optic nerve sheath fluid suspicious as papilloedema, and children were referred for immediate neurological workup.

EDI-OCT findings

PHOMS were detected in 63 out of 64 eyes of 32 children (98.4%, Table 1). The mean vertical size of PHOMS measured 469 ± 103 µm, (range 194–737). PHOMS showed a typical appearance of hyperreflective lesions surrounding the optic disc and were located subretinal and above the Bruch's membrane (Figs. 1b, d, 2b and 3b, d). In 60 eyes (93.8%), small hyperreflective foci inside the PHOMS were present (Fig. 2b, c). Moreover, we identified a distinct ring sign visible on the infrared images, corresponding clearly to the edge of the PHOMS as seen on EDI-OCT, demonstrated in Figs. 1a, c, 2a and 4a, c. This ring sign was present in all cases of PHOMS.

ONHD were present in 13 eyes (20.3%, Table 1) and appeared as hyporeflective structures with a full or partial hyperreflective margin (Fig. 3d). PHOMS co-existed with ONHD in all 13 eyes. There was no statistically significant difference in terms of age of children with and

Table 1 Descriptive statistics.

Age, years, mean ± SD (range)	9.0 ± 3.1 (5–16)
Female gender, *n* (%)	30 (46.9)
EDI-OCT	
PHOMS	63 (98.4)
ONHD	13 (20.3)
PHOMS size, µm, mean ± SD, (range)	469 ± 103 (194–737)
Hyperreflective foci inside the PHOMS	60 (93.8)
Ultrasound	
Minimal gain, dB, mean ± SD, (range)	54 ± 8.3 (30–70)
ONHD size, mm, mean ± SD, (range)	1.3 ± 0.4 (0.6–2.3)
Posterior shadowing, *n* (%)	13 (20.3)
FAF, $n = 32$ (50%)	
ONHD detected, *n* (%)	5/7
Small hyperreflective hyperautofluorescent spots	15 (46.9)

EDI-OCT enhanced imaging optical coherence tomography, *FAF* fundus autofluorescence, *ONHD* optic nerve head drusen, *PHOMS* peripapillary hyperreflective ovoid mass-like structures.

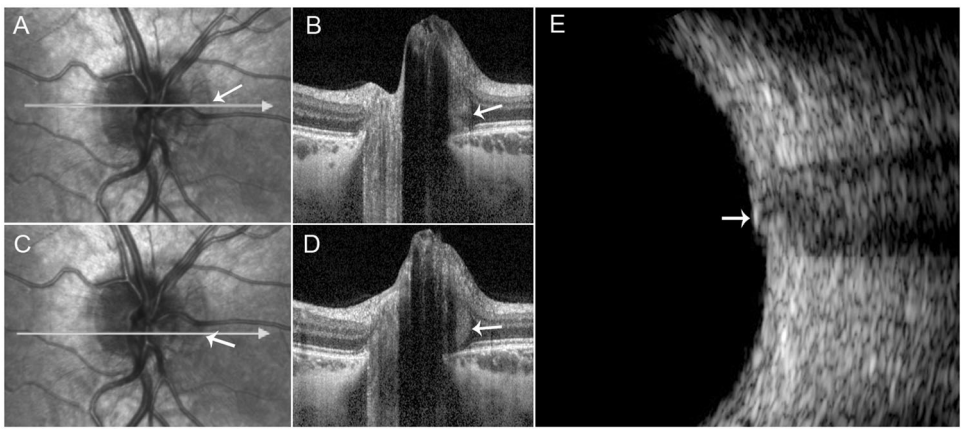

Fig. 1 Right eye of a 7-year-old boy with peripapillary hyperreflective ovoid-like mass structures. a–d Infrared images (**a**, **c**) showing a ring (arrows) nasal to the optic disc, correlating with the exact location of the peripapillary hyperreflective ovoid-like mass structures (PHOMS) edge shown on enhanced depth imaging optical coherence tomography (EDI-OCT; **b**, **d**, arrows). **e** Ultrasound B-scan showing a hyperechogenic structure (arrow) at the optic nerve head, correlating with the PHOMS seen on EDI-OCT.

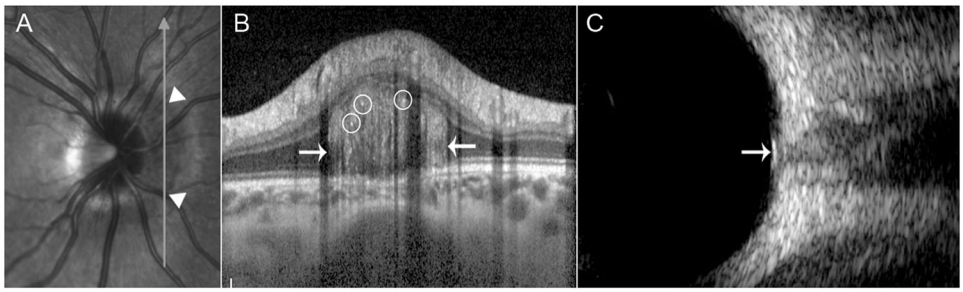

Fig. 2 Right eye of a 10-year-old boy with peripapillary hyperreflective ovoid-like mass structures. a, **b** Infrared image (**a**) showing a ring (arrows) nasal to the optic disc, correlating with the exact location of the peripapillary hyperreflective ovoid-like mass structures (PHOMS) edge shown on enhanced depth imaging optical coherence tomography (EDI-OCT) in (**b**) (arrows). The PHOMS contains small hyperreflective spots (encircled). **c** Ultrasound B-scan showing a hyperechogenic structure (arrow) at the optic nerve head, correlating with the PHOMS seen on EDI-OCT.

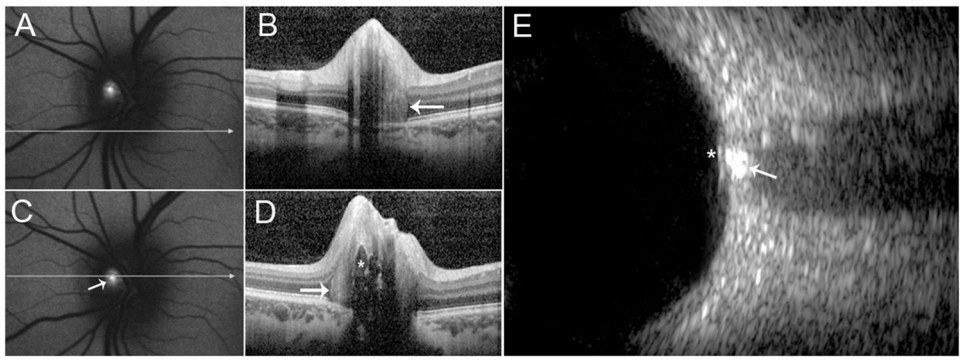

Fig. 3 Left eye of a 12-year-old girl with optic nerve head drusen and peripapillary hyperreflective ovoid-like mass structures. a, **c** Autofluorescence images showing the optic nerve head drusen (ONHD) as a hyperautofluorescent structure (arrow). **b** Enhanced depth imaging optical coherence tomography (EDI-OCT) showing peripapillary hyperreflective ovoid-like mass structures (PHOMS; arrow heads) and **d** showing the ONHD as a hyporeflective lesion with hyperreflective edge. **e** Ultrasound B-scan showing a flat superficial hyperechogenic structure (asterisk), correlating to the PHOMS and a larger deeper hyperechogenic structure correlating with the ONHD.

without ONHD (8.6 ± 2.5 vs. 9.1 ± 3.2 years, respectively; $p = 0.987$).

One eye out of the 64 did not demonstrate any abnormality on EDI-OCT.

Ultrasound

Ultrasound detected ONHD in 13 eyes with full correspondence to the OCT findings. Drusen were displayed with the typical appearance as hyperechogenic structures causing posterior shadowing (Fig. 3e). In 50 eyes (78.1%), there was only a distinct echographic picture of smaller hyperechogenic structures but no posterior shadowing (Figs. 1e, 2c, 3e and 4d), which is compatible with PHOMS alone. PHOMS appeared on ultrasound as hyperechogenic structures that were located closely to the retinal level, and not in the deeper levels of the optic nerve head. In cases with ONHD and coexisting PHOMS, the two lesions types were identified on ultrasound (Fig. 3e).

In cases of ONHD, the size of the hyperechogenic structures was significantly larger compared to those seen with PHOMS without drusen (1.61 ± 0.41 mm vs. 1.26 ± 0.37 mm, $p = 0.009$, Table 2). The mean minimal gain to appearance of all hyperechogenic structures was 54 ± 8 dB (30–70). Although the minimal gain was lower in cases with ONHD (50 ± 11 dB) compared to those with PHOMS without ONHD (56 ± 8 dB), the difference did not reach statistical significance ($p = 0.08$, Table 2).

A mild inversive nonlinear correlation was found between PHOMS size measured on EDI-OCT and minimal US gain (rs −0.256; $p = 0.048$). Moreover, the size of the hyperechogenic structures and minimal US gain were inversely lineary correlated (rp −0.470; $p < 0.001$).

Fundus autofluorescence

FAF was available in 32 eyes (50%). Out of 13 eyes with ONHD, FAF was available in 7 cases and displayed the typical appearance with confluent hyperautofluorescent areas in 5 eyes (Fig. 3a, c).

In eyes with PHOMS, we detected small hyperautofluorescent spots in the optic nerve head in 15 eyes (46.9%,

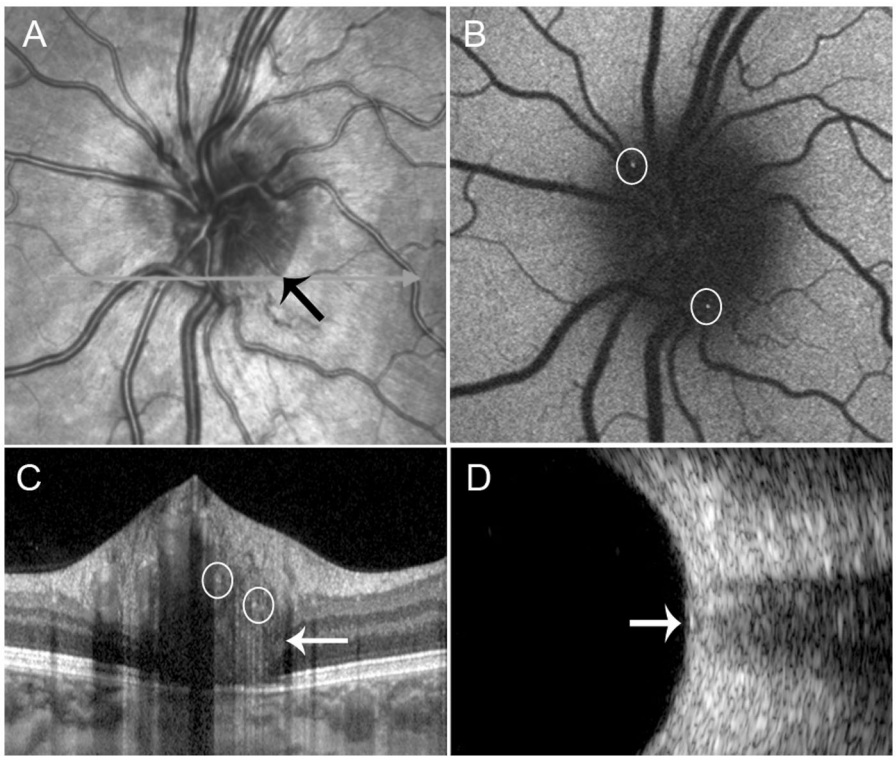

Fig. 4 Left eye of a 9-year-old girl with peripapillary hyperreflective ovoid-like mass structures. a–c Infrared image (**a**) showing a ring (arrow) temporal to the optic disc, correlating with the exact location of the peripapillary hyperreflective ovoid-like mass structures (PHOMS) edge shown on enhanced depth imaging optical coherence tomography (EDI-OCT) in (**c**) (arrow). The PHOMS contains small hyperautofluorescent spots seen on fundus autofluorescence (**b**, encircled), and hyperreflective spots on the infrared images (**c**, encircled). **d** Ultrasound B-scan showing a hyperechogenic structure (arrow) at the optic nerve head, correlating with the PHOMS seen on EDI-OCT.

Fig. 4b). Eyes with PHOMS that measured larger on EDI-OCT were more likely to display these hyperautofluorescent spots on FAF, compared to eyes with smaller PHOMS (487 ± 107 µm vs. 460 ± 91 µm, $p = 0.047$).

Remarkably, we did not identify these small hyperautofluorescent spots in eyes which had coexisting ONHD and PHOMS.

The presence of hyperautofluorescence on FAF was not correlated to patient's age ($p = 0.278$) or the size of the hyperechogenic structure seen on ultrasound ($p = 0.715$).

The interobserver reliability for grading results κ was 0.95, indicating good reliability.

Table 2 Comparison between eyes with and without optic nerve head drusen.

	With ONHD $n = 13$ (20.3%)	Without ONHD $n = 50$ (78.1%)	p value
Age, years, mean ± SD	8.6 ± 2.5	9.1 ± 3.2	0.987
Minimal ultrasound gain, dB, mean ± SD	50 ± 11	56 ± 8	0.08
ONHD ultrasound size, mm, mean ± SD	1.61 ± 0.41	1.26 ± 0.37	0.009

ONHD optic nerve head drusen, *SD* standard deviation.

Discussion

To our best knowledge, this is the first study showing that PHOMS is the most common cause of pseudopapilloedema in children. We were able to distinguish PHOMS not only on EDI-OCT, but also characterize their appearance on ultrasound, fundus autofluorescence, and infrared images. In accordance to Teixeira et al. we found distinct differences between PHOMS and ONHD in children [21].

The introduction of EDI-OCT enabled the recognition of different types and components of optic nerve head lesions causing pseudopapilloedema. *The Optic Disc Drusen Study Consortium* created a standardized and consistent definition of ONHD on OCT and introduced the distinct entity of PHOMS. Those lesion were described based on 28 cases of adult patients with proved ONHD on ultrasound which were examined by EDI-OCT [14]. The authors did not identify PHOMS on ultrasound. Interestingly, in their study all patients had coexisting ONHD which cause significant shadowing due to their high echogenicity which might have hidden the PHOMS. In contrary, 79.9% of our patients presented PHOMS without ONHD on EDI-OCT, which allowed us to study PHOMS appearance on ultrasound in the absence of drusen. We were able to identify distinct hyperechogenic structures on ultrasound in all 50 cases, correlating to the PHOMS seen on EDI-OCT. Those structures appear statistically significantly smaller than ONHD on ultrasound (1.26 ± 0.37 mm vs. 1.61 ± 0.41 mm, $p = 0.009$) and are slightly less echogenic than ONHD,

located more closely to the retinal level and do not show posterior shadowing. (Figs. 1e, 2c and 3e).

We identified small hyperreflective foci on EDI-OCT located within the PHOMS in 93.8% of the cases which might correlate to the small hyperautofluorescent spots seen on FAF (Fig. 4b, c). Our findings indicate that PHOMS might contain calcium, which is visible on the different imaging modalities in a smaller amount than in ONHD [22].

Until now, PHOMS are only an imaging diagnosis, without a confirmed pathology [10]. Malmqvist et al. hypothesized that PHOMS might correspond to lateral bulging or herniation of distended axons into the peripapillary retina [14]. Our results support the hypothesis that the different OCT appearances of PHOMS and drusen might represent a continuum in the evolution of ONHD, beginning as a hyperreflective peripapillary mass representing axoplasmic stasis. Continuing of the same process might lead to extrusion of calcified mitochondria, which were attributed to the finding of hyperreflective bands or previously called "granular" drusen on OCT [9, 13]; in the final stage, calcium deposition might lead to the appearance of hyporeflective masses with hyperreflective margins—finally defined as ONHD on OCT. Histopathologic analysis of PHOMS is still missing and might shed light on the inner compounds of these lesions.

In the addition to distinct findings for PHOMS on EDI-OCT, ultrasound and FAF, we provide an additional tool to diagnose PHOMS by using the infrared images. In all cases with PHOMS, we identified a distinct ring sign surrounding the optic nerve, correlating to the exact position of the PHOMS edge on EDI-OCT (Figs. 1a, c and 2a). Our study did not compare the infrared image findings to cases with papilloedema and hence we do not recommend relying on this sign to rule out true oedema which may suggest a serious neurologic condition. A comparative study including cases with PHOMS with and without coexisting oedema is needed in order to investigate the value of this finding in the evaluation of optic nerve head elevation.

Mean age in the current study was 9.0 ± 3.1 years (range 5–16). A study about ONHD with a median follow-up of 56 years showed only minimal overall progression over time [23]. However, a tendency towards progression in ONHD number and size was found for patients who were initially examined at younger age. Transition from buried to superficial ONHD is believed to occur during teenage years, which seems to be the period of time with most rapidly visual field defects progression [7, 23]. Lee et al. investigated ONHD using spectral-domain OCT in 99 eyes and found that patients with visible ONHD were older than those with buried drusen [11]. Their paper was published before the definition of the *Consortium* and therefore termed "subretinal hyperreflective masses" as buried drusen, supporting our findings.

As prospective data about the change or progression of PHOMS are missing, closer follow-up including visual field examination in younger children might be advisable. In our cohort, there were no cases of increased intracranial pressure (ICP), and we did not identify excess optic nerve sheath fluid on ultrasound [20]. All children included in this study underwent B-scan echography and we did not identify evidence of excess optic nerve sheath fluid (seen as a hypoechogenic crescent sign surrounding the optic nerve head) in any case. In these cases we do not perform routine A-scan echography to measure the optic nerve sheath width. However, in all suspect cases A-scan should we performed with an upper limit of 3.0 mm for normal values [20]. While ultrasound is a valuable tool for detecting signs of increased ICP, further workup should be initiated in all suspect cases.

As PHOMS have been described in the setting of idiopathic intracranial hypertension [14], further investigation with long-term follow-up in a prospective manner in a large paediatric population is needed. While the prevalence of PHOMS in a general population of children has not been investigated, it has been shown to be associated with myopic shift in children [24].

PHOMS was found to be the most common cause for pseudopapilloedema in this paediatric cohort. Ultrasound was not found to be an appropriate imaging modality for that entity. PHOMS is a new entity of optic nerve head lesions and their evolution over years is unknown. As it might be a precursor of buried ONHD, we recommend that after having ruled out true papilloedema using ultrasound (i.e., excess optic nerve sheath fluid), EDI-OCT should be performed, in order not to miss PHOMS. Follow-up after children with PHOMS, using EDI-OCT and visual fields, is important since development of drusen is associated with a variety of secondary complications such as visual field defects, haemorrhages and CNV.

Summary

What was known before

- Suspected papilloedema is a common cause for referral of child.
- PHOMS characteristics have not been described in a comprehensive manner in a paediatric population.

What this study adds

- This is the first study showing that PHOMS are the most common cause for pseudopapilloedema in children.
- PHOMS is a new entity of optic nerve head lesions. It might be a precursor of buried optic nerve head drusen.

- This study offers new tools to identify and follow-up these lesions early in childhood using EDI-OCT.

Funding This research received no specific grant from any funding agency in the public, commercial or not-for-profit sectors.

Compliance with ethical standards

Conflict of interest The authors declare that they have no conflict of interest.

Publisher's note Springer Nature remains neutral with regard to jurisdictional claims in published maps and institutional affiliations.

References

1. Kovarik JJ, Doshi PN, Collinge JE, Plager DA. Outcome of pediatric patients referred for papilledema. J AAPOS. 2015;19:344–8.
2. Chang MY, Pineles SL. Optic disk drusen in children. Surv Ophthalmol. 2016;61:745–58.
3. Leon M, Hutchinson AK, Lenhart PD, Lambert SR. The cost-effectiveness of different strategies to evaluate optic disk drusen in children. J AAPOS. 2014;18:449–52.
4. Mishra A, Mordekar SR, Rennie IG, Baxter PS. False diagnosis of papilloedema and idiopathic intracranial hypertension. Eur J Paediatr Neurol. 2007;11:39–42.
5. Erkkila H. Clinical appearance of optic disc drusen in childhood. Albrecht Von Graefes Arch Klin Exp Ophthalmol. 1975;193:1–18.
6. Auw-haedrich C, Staubach F, Witschel H, Breisgau F. Optic disk drusen. Surv Ophthalmol. 2002;47:515–32.
7. Frisen L, Frise L, Frisen L. Evolution of drusen of the optic nerve head over 23 years. Acta Ophthalmol. 2008;86:111–2.
8. Spencer TS, Katz BJ, Weber SW, Digre KB. Progression from anomalous optic discs to visible optic disc drusen. J Neuroophthalmol. 2004;24:297–8.
9. Sato T, Mrejen S, Spaide RF. Multimodal imaging of optic disc drusen. Am J Ophthalmol. 2013;156:275–282.e1.
10. Gise R, Gaier ED, Heidary G, Gise R, Gaier ED, Heidary G. Diagnosis and imaging of optic nerve head drusen diagnosis and imaging of optic nerve head drusen. Semin Ophthalmol. 2019;0:1–8. https://doi.org/10.1080/08820538.2019.1620804.
11. Lee KM, Woo SJ, Hwang J-M. Morphologic characteristics of optic nerve head drusen on spectral-domain optical coherence tomography. Am J Ophthalmol. 2013;155:1139–1147.e1.
12. Silverman AL, Tatham AJ, Medeiros FA, Weinreb RN. Assessment of optic nerve head drusen using enhanced depth imaging and swept source optical coherence tomography. J Neuro-Ophthalmol. 2015;34:198–205.
13. Traber GL, Weber KP, Sabah M, Keane PA, Plant GT. Enhanced depth imaging optical coherence tomography of optic nerve head drusen a comparison of cases with and without visual field loss. Ophthalmology. 2016;124:66–73.
14. Malmqvist L, Bursztyn L, Costello F, Digre K, Fraser JA, Fraser C, et al. The optic disc drusen studies consortium recommendations for diagnosis of optic disc drusen using optical coherence tomography. J Neuro-Ophthalmol. 2017;38:299–307.
15. Merchant KY, Su D, Park SC, Qayum S, Banik R, Liebmann JM, et al. Enhanced depth imaging optical coherence tomography of optic nerve head drusen. Ophthalmology. 2012;120:1409–14.
16. Slotnick S, Sherman J. Disc drusen. Ophthalmology. 2012;119:652–652.e1.
17. Lee KM, Woo SJ, Hwang J-M. Differentiation of optic nerve head drusen and optic disc edema with spectral-domain optical coherence tomography. Ophthalmology. 2011;118:971–7.
18. Chang MY, Velez FG, Demer JL, Bonelli L, Quiros PA, Arnold AC, et al. Accuracy of diagnostic imaging modalities for classifying pediatric eyes as papilledema versus pseudopapilledema. Ophthalmology. 2017;124:1839–48.
19. Kulkarni KM, Pasol J, Rosa PR, Lam BL. Differentiating mild papilledema and buried optic nerve head drusen using spectral domain optical coherence tomography. Ophthalmology. 2014;121:959–63.
20. Neudorfer M, Ben-Haim MS, Leibovitch I, Kesler A. The efficacy of optic nerve ultrasonography for differentiating papilloedema from pseudopapilloedema in eyes with swollen optic discs. Acta Ophthalmol. 2013;91:376–80.
21. Teixeira FJ, Marques RE, Mano SS, Couceiro R, Pinto F. Optic disc drusen in children: morphologic features using EDI-OCT. Eye. 2019. https://doi.org/10.1038/s41433-019-0694-6; https://pubmed.ncbi.nlm.nih.gov/31745329.
22. McNicholas MM, Power WJ, Griffin JF, Funduscopic W, Normal A. Sonography imaging findings when funduscopic in optic disk drusen: and role in diagnosis findings are normal. Am J Roentgenol. 1994;162:161–3.
23. Malmqvist L, Lund-Andersen H, Hamann S. Long-term evolution of superficial optic disc drusen. Acta Ophthalmol. 2017;95:352–6.
24. Lyu IJ, Park K-A, Oh SY. Association between myopia and peripapillary hyperreflective ovoid mass-like structures in children. Sci Rep. 2020;10:2238.